environmental microbiology

Environmental Microbiology (2020) **00**(00), 00–00 doi:10.1111/1462-2920.15123

Special Issue Article

A universal oyster infection model demonstrates that *Vibrio vulnificus* Type 6 secretion systems have antibacterial activity *in vivo*

Cameron L. Hubert* **and Stephen Ll. Michell*** *College of Life and Environmental Sciences, University of Exeter, Exeter, EX4 4QD, UK.*

Summary

With the rapid increase of aquaculture contributing to sustainable food security, comes the need to better understand seafood associated diseases. One of the major aquatic bacterial genera responsible for human infections from seafood is *Vibrio*, especially from oysters. Currently, *in vivo* study of bacterial interactions within oysters is limited by the inability to promote high-level uptake of bacteria by oysters. This study has therefore evolved current natural marine snow protocols to generate 'artificial' marine snow, into which bacteria can be incorporated to facilitate extensive uptake by oysters. This presents an adaptable model for bacterial study within filter-feeding shellfish. Using this model, we demonstrate for the first time the antibacterial activity of *Vibrio vulnificus* Type 6 secretion systems *in vivo*, revealing an important role for the T6SS in *V. vulnificus* ecology.

Introduction

The State of the World Fisheries and Aquaculture (SOFIA) report (2018) describes 80 million tonnes of aquaculture produced in 2016, of which molluscs totalled 17.1 million tonnes (SOFIA, 2018). Comprising 47% of global fish and mollusc production, fisheries and aquaculture are paramount food security concerns for ensuring continued and consistent seafood production. However, aquaculture practices are becoming increasingly intensive to meet this demand, resulting in proliferation of marine pathogens and food safety issues (Bondad-Reantaso *et al*., 2005; Rico *et al*., 2012). *Vibrio* species are a major hurdle in bivalve production, in particular oysters, due to their mortality in early developmental stages and their deleterious impact on adult shellfish (Dubert *et al*., 2016; Bruto *et al*., 2017). Seasonal losses to the oyster pathogen, *Vibrio splendidus*, have consistently reached up to 80% in oyster farms in the Bay of Morlaix over a 10-year span (Lacoste *et al*., 2001). Furthermore, the *Vibrionaceae* family harbours numerous human pathogens, including *Vibrio vulnificus*, *Vibrio cholerae* and *Vibrio parahaemolyticus*, which are responsible for around 80,000 vibriosis cases annually in the United States (CDC, n.d.). The investigation of *Vibrio* ecology is therefore essential for understanding how to best manage the threat they pose to aquaculture and human health.

Studies exploring bacterial behaviour within shellfish have previously utilized oysters inoculated through exposure to water supplemented with bacterial culture (Srivastava *et al*., 2009; Pu *et al*., 2018). However, this approach is limited by inefficient uptake of bacteria as oysters filter and ingest particles based primarily on size (Froelich *et al*., 2013). Planktonic *V. vulnificus* (2 μm) fall below the optimal size range for ingestion, therefore only achieving low levels of uptake in such experiments (Froelich and Noble, 2014). Incorporation of bacterial cultures into larger, naturally forming aggregates known as 'marine snow' has shown potential as a method for enhancing bacterial uptake by oysters (Froelich *et al*., 2013). Marine snow is composed of diatoms, faecal matter, microorganisms, protists and other miscellaneous elements brought together at random that present a unique environment for bacterial colonization and survival. However, this stochastic process generates inherent variability (Kiørboe *et al*., 1990; Grossart *et al*., 2003; Kiørboe *et al*., 2003; Passow *et al*., 2012).

Vibrio vulnificus is the leading cause of seafood-related disease in the United States and is increasing in prevalence globally, correlating with rising sea-surface temperatures (Jones and Oliver, 2009; Baker-

Received 30 April, 2020; revised 1 June, 2020; accepted 7 June, 2020. *For correspondence. E-mail ch524@exeter.ac.uk; s.l.michell@exeter.ac.uk, Tel. +44(0)1392725524

Austin *et al*., 2012; Vezzulli *et al*., 2015; Baker-Austin *et al*., 2017; Deeb *et al*., 2018). Ingestion can result in severe gastroenteritis which may develop into primary septicaemia, with symptoms including vomiting, haemorrhagic bullae, secondary lesions on extremities and severe hypotension (Beatty *et al*., 2017). Progression to primary septicaemia results in 50% patient fatality within 48 h of hospital admission (Chiang *et al*., 2003). Exposure of open wounds to contaminated water results in erythema, haemorrhagic bullae, cellulitis and intense pain (Oliver, 2005). Failing immediate treatment, infected lesions frequently turn necrotic. While visually more aggressive, wound infections carry a lower mortality rate of 25% compared with ingestion whose rates are >50% if treated within 24 h and 100% if untreated for over 72 h (Jones and Oliver, 2009; Kim *et al*., 2011). Particularly at risk are patients with compromised immune systems, liver disease and haematological disorders, with 80% of patients already presenting at least one pre-existing medical condition (Menon *et al*., 2014).

Studies comparing the genetic makeup of *V. vulnificus* strains identified two Type 6 secretion systems (T6SSs) labelled T6SS1 and T6SS2 (Church *et al*., 2016). A molecular syringe composed of 13 essential proteins, the T6SS functions to inject cytotoxic effectors into neighbouring cells (Ho *et al*., 2014). Shown to have a wide range of activity in other bacterial species, the T6SS has been implicated in both anti-prokaryotic and anti-eukaryotic activity (Salomon *et al*., 2013; Ray *et al*., 2017; Trunk *et al*., 2018; Berni *et al*., 2019). Interestingly, whilst the T6SS2 was identified in all *V. vulnificus* strains sequenced to date, only some strains possessed the T6SS1. *in vitro* competition assays showed that T6SS1-positive (T6SS1$^+$) strains were able to target and kill T6SS-negative (T6SS1$^-$) strains as well as other bacterial species. T6SS-mediated antibacterial activity has been demonstrated by a range of bacteria, such as *Klebsiella pneumoniae*, *V. cholerae* and *Vibrio fluvialis*, in various *in vivo* models including mice, rabbits and squid (Fu *et al*., 2018; Speare *et al*., 2018; Hsieh *et al*., 2019). It was thus hypothesised that the T6SS1 may play a significant role in competition between *Vibrios*, and on bacterial population dynamics *in vivo*.

Here we demonstrate that *V. vulnificus* T6SS1 and T6SS2 mediate antibacterial activity in an oyster *in vivo* model. Killing was shown to be thermoregulated with only T6SS1 active at 30°C, but both T6SS1 and T6SS2 active at 21°C. This is the first study to present a role for the T6SS2 of *V. vulnificus*. For *in vivo* studies, we have adapted current marine snow methodologies to develop a defined, highly controllable 'artificial marine snow' (AMS) based on aggregation of the diatom species, *Thalassiosira pseudonana*. Using inoculated AMS, we achieved higher uptake of *V. vulnificus* and *Salmonella enterica* serovar Enteritidis by oysters than any study to date. We believe this methodology may have much broader application within research and aquaculture. Co-culture of strains within oysters showed that T6SS1 and T6SS2 mediate intra- and inter-species competition *in vivo* and may play a pivotal role in the establishment of *V. vulnificus* strains within filter-feeding shellfish and subsequent prevalence of virulent strains.

Results

Vibrio vulnificus *T6SSs display no anti-eukaryotic activity against* Dictyostelium discoideum

The T6SS of *V. cholerae* demonstrates a range of anti-eukaryotic functionality, such as actin cross-linking to inhibit phagocytosis by macrophages (Pukatzki *et al*., 2007). We hypothesised that *V. vulnificus* T6SSs may also possess anti-eukaryotic activity. To explore this hypothesis, wild-type *V. vulnificus* 106-2A (T6SS1$^+$/T6SS2$^+$) and mutants of both T6SSs were employed in *Dictyostelium discoideum* plaque-forming assays. T6SS1 and T6SS2 mutants were generated through in-frame deletion of *hcp1* and *hcp2* genes encoding effector-transporting needle components of the T6SS (Fig. 1A) (Cascales and Cambillau, 2012). Mutants were labelled ΔT6SS1 (*hcp1*$^-$) and ΔT6SS2 (*hcp2*$^-$) respectively. Deletion of *hcp1* and *hcp2* was confirmed via PCR and expression of downstream genes verified by reverse-transcriptase-PCR (RT-PCR) (Fig. 1B and C). For *D. discoideum* plaque-forming assays, wild-type *V. vulnificus* 106-2A and T6SS deletion mutants were combined with predatory *D. discoideum* AX3 and plated as a lawn on SM agar for 3–5 days at 21°C. If the T6SSs possess anti-eukaryotic activity, larger plaques of predation should be observed relative to wild-type *V. vulnificus* 106-2A following their deletion. No plaques were observed on plates containing wild-type *V. cholerae* V52, a strain with previously characterized anti-eukaryotic activity (Fig. 1D) (Miyata *et al*., 2011). However, visible plaques were recorded on *V. vulnificus* 106-2A, ΔT6SS1 (*hcp1*$^-$) and ΔT6SS2 (*hcp2*$^-$) lawns, indicative of *V. vulnificus* predation by *D. discoideum* (Fig. 1E–G). Measurement of plaque diameter showed no significant difference in predation efficiency between *V. vulnificus* strains (Fig. 1H). These results indicate that the T6SSs of *V. vulnificus* are unable to target *D. discoideum* and have no observable anti-eukaryotic activity at 21°C in this model of infection. A similar lack of anti-eukaryotic activity has also been previously demonstrated in a *Galleria mellonella* model of virulence at 37°C (Church *et al*., 2016).

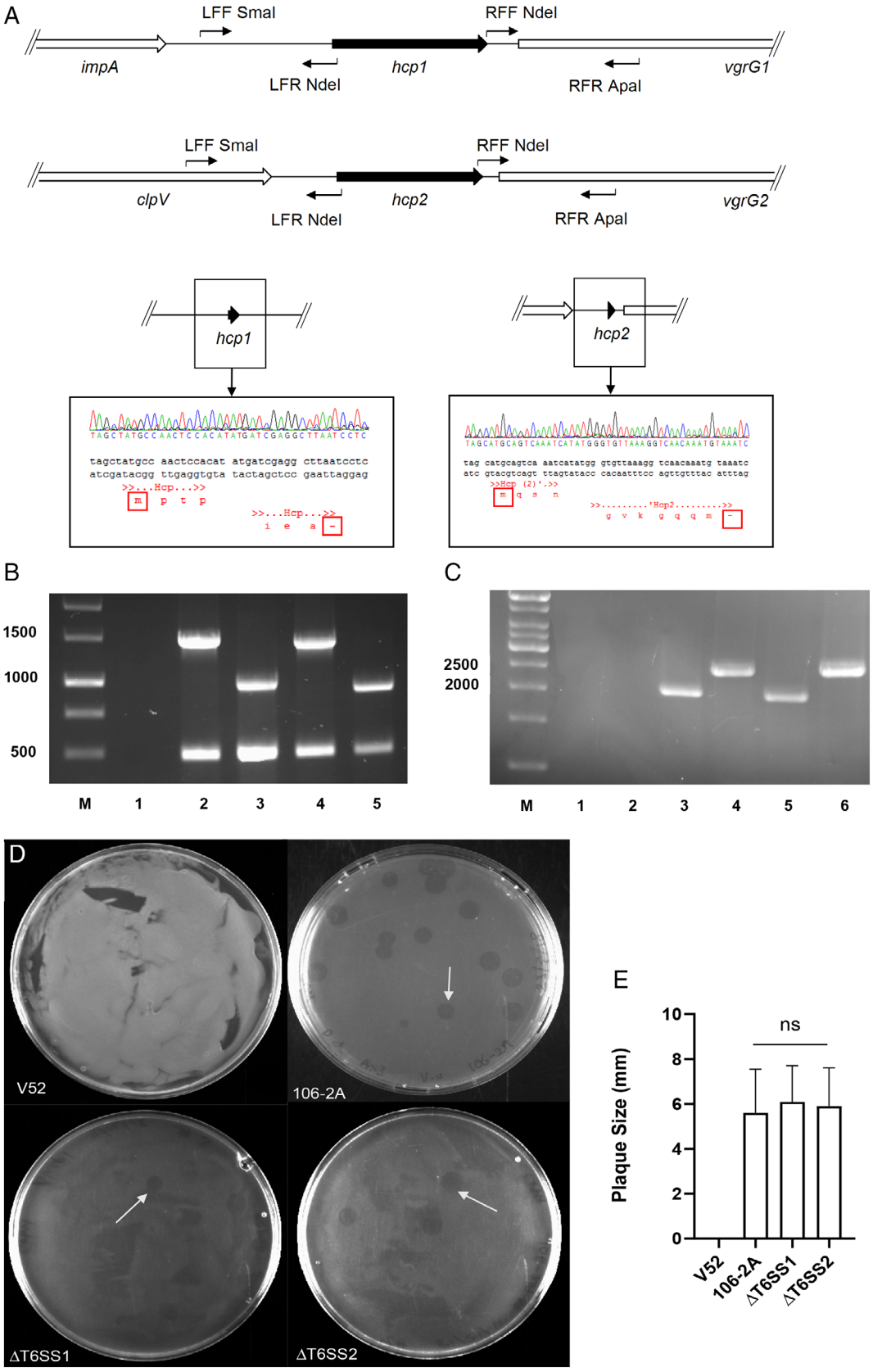

Both V. vulnificus *T6SS1 and T6SS2 demonstrate* in vitro *antibacterial activity at environmental temperatures*

Given the apparent lack of anti-eukaryotic phenotype from either of the T6SSs of *V. vulnificus* against *D. discoideum*, we sought to further investigate previous observations of *V. vulnificus* intra- and inter-species competition mediated by the T6SS (Church *et al*., 2016). As T6SS activation in *V. cholerae* has been identified at 23°C, we aimed to explore whether *V. vulnificus* also exhibits T6SS activity at environmental temperatures (Ishikawa *et al*., 2012). Competition assays were thus conducted at 21°C, an optimal temperature for *V. vulnificus* growth in sea water (Kaspar and Tamplin, 1993). To facilitate enumeration of strains in competition, attacker strains *V. vulnificus* 106-2A (wild-type), ΔT6SS1 (*hcp1*$^{-}$) and ΔT6SS2 (*hcp2*$^{-}$) were transformed with pVv3-Kan to confer kanamycin resistance (Klevanskaa *et al*., 2014). Likewise, an environmental 'prey' *V. vulnificus* strain, 99-743, (T6SS1^{-}, T6SS2^{+}), was transformed with pVv3-Tmp to confer trimethoprim resistance.

Competition between attacker and prey *V. vulnificus* confirms T6SS1 activity at 30°C, demonstrated by a clear and significant 1000-fold reduction of prey 99-743 following co-culture with 106-2A but no reduction when cultured with ΔT6SS1 (*hcp1*$^{-}$) (Fig. 2A). We therefore sought to see if a more environmentally representative temperature had an effect on T6SS activity. Competition assays were thus conducted at 21°C for both T6SS deletion strains (Fig. 2B). We observed a significant 10-fold reduction in 99-743 prey counts following individual co-culture with 106-2A and the ΔT6SS2 (*hcp2*$^{-}$) mutant at 21°C. In addition, at 21°C we also observed for the first time a T6SS2 antibacterial activity, manifested as a reduction in prey numbers comparable with that observed for the T6SS1 ($p < 0.05$) (Fig. 2B). To confirm that the observed reduction in prey numbers were indeed T6SS-dependent and not the result of alternative antibacterial mechanisms active at 21°C, a 106-2A Δ*hcp1*Δ*hcp2* double mutant was generated, named ΔT6SS1/2. No reduction in recovery of the prey strain 99-743 was observed following co-culture with ΔT6SS1/2 (*hcp1*$^{-}$, *hcp2*$^{-}$). These data confirm that killing by ΔT6SS1 (*hcp1*$^{-}$) and ΔT6SS2 (*hcp2*$^{-}$) was due to the T6SS2 and T6SS1, respectively, and that both systems are capable of intra-species targeting at 21°C *in vitro*. Given the broad nature of T6SS activity, we investigated whether the T6SS competent strains of *V. vulnificus* were able to demonstrate inter-species antibacterial activity. To address this question, we utilized *Salmonella* Enteritidis CC012 as a prey strain in competition with our panel of attacker *V. vulnificus* T6SS mutants. Similar to our intra-species data, we observed a T6SS1-driven 1000-fold reduction of prey CC012 at 30°C but no reduction with the ΔT6SS1 (*hcp1*$^{-}$) attacker strain (Fig. 2C). Of interest, the competition assays at 21°C demonstrated that CC012 was targeted by 106-2A, ΔT6SS1 (*hcp1*$^{-}$) and ΔT6SS2 (*hcp2*$^{-}$), resulting in significantly reduced prey recovery ($p < 0.01$) (Fig. 2D). This reduction was not observed when co-cultured with the double mutant, ΔT6SS1/2 (*hcp1*$^{-}$, *hcp2*$^{-}$), reinforcing the role of *V. vulnificus'* T6SS2 in bacterial killing at environmental temperatures.

Development of a delivery model to facilitate reproducible uptake of bacteria by oysters

Having demonstrated *V. vulnificus* T6SS activity *in vitro*, we sought to investigate whether such activity occurred *in vivo* by developing an oyster model for studying bacterial interactions. Previous *in vivo* models of bacterial uptake utilizing oysters have either employed directly inoculated sea water or 'natural marine snow' (NMS) (Srivastava *et al*., 2009; Froelich *et al*., 2013; Pu *et al*., 2018). Our attempt at incorporating *V. vulnificus* into NMS, formed by aggregating seawater particulate matter, showed some success but did not achieve incorporation $>3 \times 10^4$ CFU/g marine snow (Fig. 3A). This may be due to the competition from the naturally occurring bacteria that pre-colonize the particulate matter preventing *V. vulnificus* establishment. We showed that NMS contained diverse bacterial populations, including *Vibrio* species, as determined by growth on both LB and Thiosulfate-Citrate-Bile Salts-sucrose (TCBS) agar plates (Fig. 3A). Moreover, our NMS also varied by size and composition (Fig. S1). Given that the levels of

Fig. 1. Generation of *Vibrio vulnificus* 106-2A T6SS deletion mutants, ΔT6SS1 and ΔT6SS2, for *Dictyostelium discoideum* plaque-forming assays. A. Schematic view of *V. vulnificus* 106-2A Hcp1 and Hcp2 regions with marked primer-binding sites. Left and right flanking regions of *hcp1* and *hcp2* were ligated for construction of in-frame deletion cassettes. Deletion cassettes were introduced to *V. vulnificus* 106-2A using pDM4 to generate ΔT6SS1 (*hcp1*$^{-}$) and ΔT6SS2 (*hcp2*$^{-}$). Truncated *hcp1* and *hcp2* genes from *V. vulnificus* ΔT6SS1 and *V. vulnificus* ΔT6SS2 are shown below with confirmatory sequencing data. Start and stop codons for *hcp1* and *hcp2* are highlighted with red boxes.
B. PCR confirmation of *hcp1* and *hcp2* deletion. M – molecular marker (bp), 1 – no template control, 2 – *hcp1* positive control, 3 – ΔT6SS1 mutant, 4 – *hcp2* control, 5 – ΔT6SS2 mutant. Lanes 2–5 also exhibit a species-specific *vvhA* band at 500 bps to confirm mutants are *V. vulnificus*. C. Expression of genes downstream of *hcp1* and *hcp2* (*vgrG1* and *clpV* respectively) was confirmed using RT-PCR. M – molecular marker (bp), 1 – no template control, 2 – no reverse-transcriptase gDNA control, 3 – 106-2A wild-type positive *vgrG1* control, 4 – 106-2A wild-type positive *clpV* control, 5 – ΔT6SS1 *vgrG1*, 6 – ΔT6SS2 *clpV*. D. *Dictyostelium discoideum* cultures were combined with *Vibrio cholerae* V52, *V. vulnificus* 106-2A, *V. vulnificus* ΔT6SS1 and *V. vulnificus* ΔT6SS2. Example plaques are indicated with white arrows. E. Measurement of *D. discoideum* plaques ($n = 4$) following growth on *V. vulnificus* 106-2A, ΔT6SS1, ΔT6SS2 and *V. cholerae* V52. Ns – not significant.

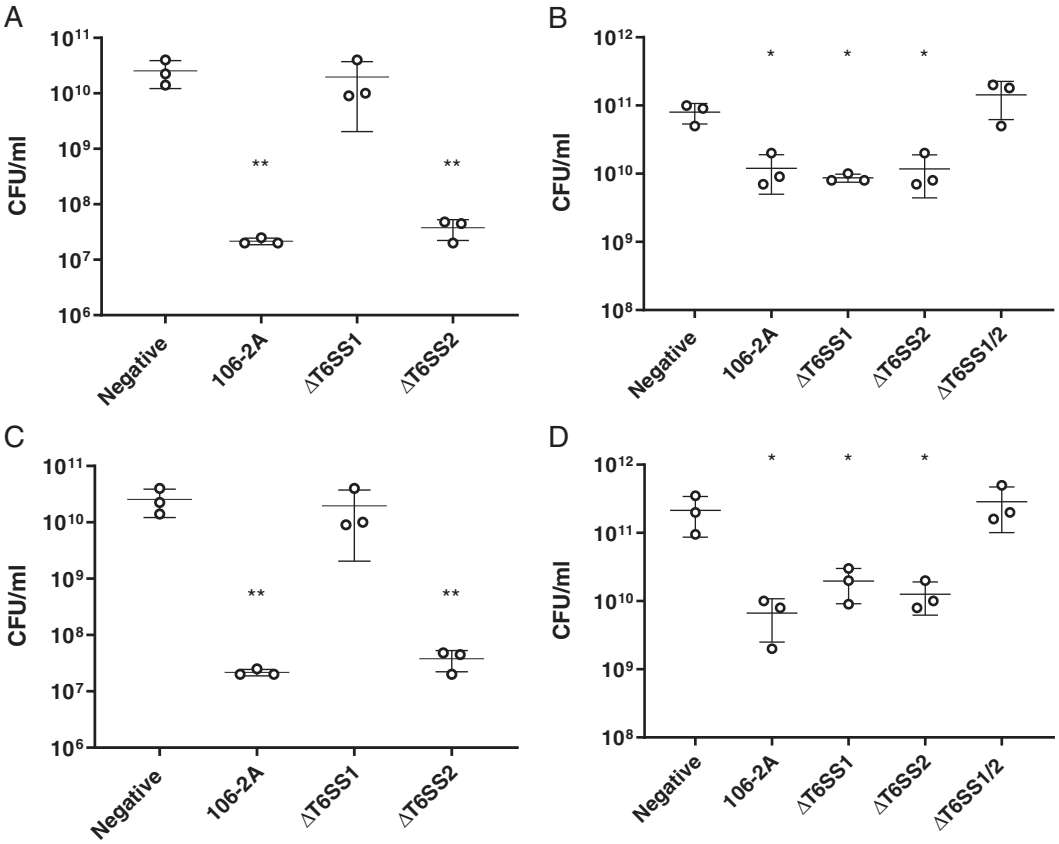

Fig. 2. Intra-/inter-species killing activity of *Vibrio vulnificus* 106-2A T6SS1 and T6SS2 at 21°C and 30°C *in vitro*. A. Viable cell counts of prey *V. vulnificus* 99-743 following co-culture with LB (negative control), *V. vulnificus* 106-2A, ΔT6SS1 or ΔT6SS2 at 30°C for 5 h. B. Viable cell counts of prey *V. vulnificus* 99-743 following co-culture with LB, *V. vulnificus* 106-2A, ΔT6SS1, ΔT6SS2 or ΔT6SS1/2 at 21°C for 24 h. C. Viable cell counts of prey *Salmonella* Enteritidis CC012 following co-culture with LB, *V. vulnificus* 106-2A, ΔT6SS1 or ΔT6SS2 at 30°C for 5 h. D. Viable cell counts of prey *S*. Enteritidis CC012 following co-culture with LB, *V. vulnificus* 106-2A, ΔT6SS1, ΔT6SS2 or ΔT6SS1/2 at 21°C for 24 h. Horizontal lines represent the mean, error bars represent the standard deviation. Assays were performed in triplicate ($n = 3$). Prey counts following co-culture with attacking strains were statistically compared with prey counts following co-culture with just LB using a one-way analysis of variance with Dunnett's corrections for multiple comparisons. * $p < 0.05$, ** $p < 0.01$.

incorporation into NMS were $<3 \times 10^4$ CFU/g marine snow and *Vibrio* levels in oysters can be up to 5×10^4 CFU/g tissue in areas where *V. vulnificus* infections are prevalent, it was clear that uptake material containing far higher numbers of *Vibrio* was required (Froelich *et al*., 2017).

To facilitate reproducible, high-level uptake of bacteria by oysters, we developed an AMS model, exploiting a natural food source for oysters. Commercial shellfish are often reared on microalgae concentrates and we therefore investigated whether bacteria could be rationally incorporated into this material. Essentially, our AMS model is the aggregation of the diatom species *T. pseudonana* CCMP 1335, with the subsequent incorporation of bacteria as detailed in the Experimental procedures section. This model reliably and reproducibly demonstrated levels of bacterial incorporation of $>10^7$ CFU/g AMS (Fig. 3B). These levels were observed for *V vulnificus* 106-2A, 99-743 and *S*. Enteritidis CC012. To control for the presence of contaminating bacteria in the *T. pseudonana*, AMS was plated on LB, *Vibrio*-selective TCBS and *Salmonella*-selective ChromoSelect agar. The remarkably high levels of bacterial incorporation into AMS, observed by plate count enumeration, contrasted starkly to the levels of incorporation into the NMS, the latter being of four orders of magnitude less than the $>10^7$ CFU/g AMS levels. Both *V. vulnificus* 99-743 and *S*. Enteritidis CC012 demonstrated significantly greater incorporation into AMS than *V. vulnificus* 106-2A ($p < 0.05$ and $p < 0.0001$ respectively). Given that we want to explore intra and inter-species competition, it was necessary to generate AMS with similar levels of bacterial strains. This was achieved simply by inoculating the starting material with appropriately higher numbers of bacterial cultures, resulting in AMS of consistent bacterial loads (Fig. 3C). Co-incorporation of attacker and prey bacteria into AMS confirmed that there was no significant killing of prey bacteria occurring in AMS that may impact

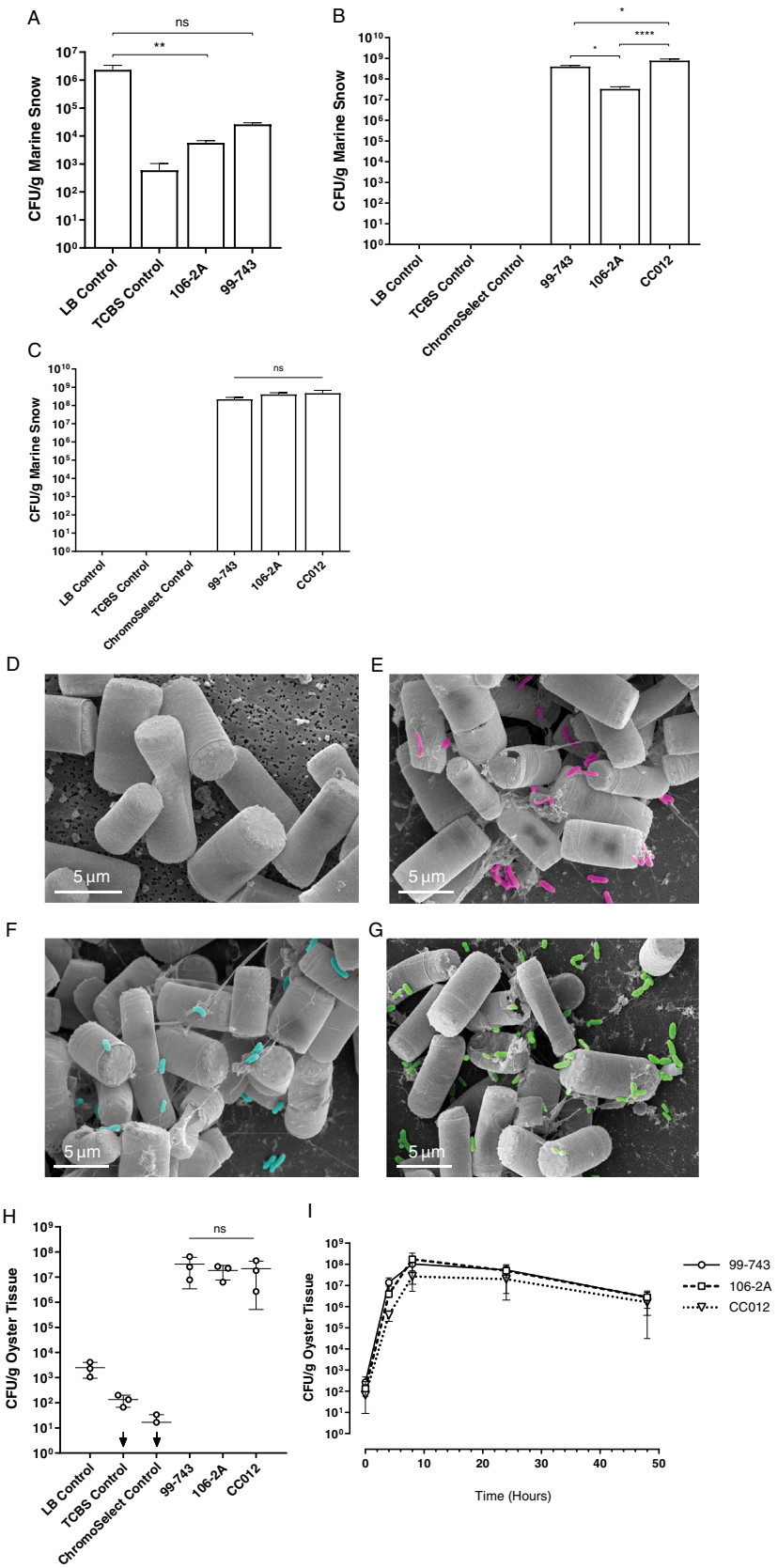

Fig. 3. Incorporation of *Vibrio vulnificus* 106-2A, 99-743 and *Salmonella* Enteritidis CC012 into AMS. A. Incorporation of *V. vulnificus* 106-2A and 99-743 into NMS generated using seawater as a substrate (n = 3). Bacteria-free controls were plated on LB and TCBS agar. B. Incorporation of *V. vulnificus* 106-2A, 99-743 and *S.* Enteritidis CC012 into AMS for 24 h at 21°C (n = 3). C. Enumeration of *V. vulnificus* 106-2A, 99-743 and *S.* Enteritidis CC012 from AMS following adjustment of starting culture concentrations to ensure equal incorporation of all strains (n = 3). D. Bacteria-free AMS control, magnification, ×5000. E. *Vibrio vulnificus* 106-2A (pink), magnification, ×4000. F. *Vibrio vulnificus* 99-743 (blue), magnification, ×4000. G. *Samonella* Enteritidis CC012 (green), magnification, ×4000. H. Oyster uptake of AMS inoculated *V. vulnificus* 106-2A, 99-743, or *S.* Enteritidis CC012. Each point represents the mean of six technical oyster replicates (n = 3), error bars show the standard deviation. Control oysters exposed to bacteria-free AMS were plated on LB, TCBS and ChromoSelect agar. Samples in which bacterial load fell below the limit of detection of 100 CFU/g oyster tissue are indicated by a downward arrow. I. Bacterial ingestion was measured over 48 h. Oysters were enumerated at T_0, T_4, T_8, T_{24} and T_{48} h (n = 3). Error bars represent the standard deviation. Statistics were performed using either a one-way analysis of variance (ANOVA) with Dunnett's corrections for multiple comparisons (Fig. 1A–C) or a nested one-way ANOVA with Dunnett's corrections for multiple comparisons (Fig. 1H). Ns – not significant, * $p < 0.05$, ** $p < 0.01$, **** $p < 0.0001$.

downstream assays (Fig. S2). AMS-incorporating bacteria were also imaged via scanning electron microscopy (SEM). *Vibrio vulnificus* 106-2A (blue), *V. vulnificus* 99-743 (pink) and *S.* Enteritidis CC012 (green) are clearly incorporated into *T. pseudonana* AMS (Fig. 3D–G).

Given the effectiveness of the developed AMS model, the next step was to investigate the suitability of this material for uptake by oysters. Oysters were exposed to inoculated AMS for 24 h at 21C. Following exposure, oyster stomachs were removed and homogenized for bacterial enumeration by plate counts. Figure 3H presents viable cell counts of *V. vulnificus* 99-743, 106-2A and *S.* Enteritidis CC012 in CFU/g tissue. To account for oyster variability, six oysters were utilized per replicate ($n = 3$). Control oysters were exposed to bacteria-free AMS and plated on LB, TCBS and ChromoSelect agar. Results showed low levels of naturally occurring microorganisms in all tested oysters (10^2–10^4 CFU/g tissue). Colony counts on TCBS and ChromoSelect agar determined that natural *Vibrio* and *Salmonella* levels were typically <1000 CFU/g and <100 CFU/g tissue respectively. Reassuringly, colony counts following exposure to inoculated AMS demonstrated highly successful uptake of both *V. vulnificus* and *S.* Enteritidis with levels of between 10^6 and 10^8 CFU/g tissue consistently recovered. Furthermore, no strain demonstrated significantly greater uptake than other strains being tested. Oyster uptake of AMS was assessed over 48 h (Fig. 3I). Rapid initial uptake was observed for all strains, with oysters showing 10^5–10^7 CFU/g tissue at T_4. Ingested concentrations rose to 10^7–10^8 CFU/g tissue at T_8; however, between T_8 and T_{48} there was no increase in bacterial uptake. While we observed $\sim 10^2$ CFU/g tissue at T_0 consisting of naturally occurring bacteria in the negative controls, this was not deemed a problem due to the significantly higher volumes resulting from exposure to inoculated aggregates.

Demonstration of controlled intra and inter-bacterial species killing in vivo *facilitated by AMS*

The aim of this study was to replicate *in vitro* competition assay data in an *in vivo* oyster model utilizing our AMS. Oysters were exposed to bacteria-free AMS and AMS containing individual attacker and prey bacterial cultures at 21°C for 24 h. These controls were enumerated by plating on LB and TCBS agar (Fig. 4A and B). Single culture controls demonstrated no significant difference in uptake between the attacker and prey strains. For the killing assays, oysters were exposed to separate AMS suspensions inoculated with either attacker or prey strains at final attacker to prey ratios of 5:1 and 10:1. Bacterial incorporation into AMS was adjusted to ensure oysters were exposed to the required attacker to prey ratios. *in vivo* co-culture of the prey strain 99-743 with either ΔT6SS1 or ΔT6SS2 resulted in significantly reduced recovery of 99-743 compared with the 99-743-only control oyster cohort ($p < 0.001$) (Fig. 4A). Typically, there was a reduction in viable counts from $>10^7$ to $<10^6$ CFU/g tissue. These reductions in numbers of prey are similar to those obtained with wild-type 106-2A as the attacker strain. To confirm that these *in vivo* levels of reduction of prey bacteria manifested by ΔT6SS1 and ΔT6SS2 were not attributable to alternative killing mechanisms, the assay was conducted using the double T6SS mutant, ΔT6SS1/2. Excitingly, we saw no significant impact on 99-743 viability when challenged with the ΔT6SS1/2 attacker strain compared with the wild-type 106-2A attacker strain. This striking observation demonstrates that the killing observed by attacker strains ΔT6SS1 and ΔT6SS2 is a consequence of the remaining T6SS. These data strongly support the hypothesis that both the T6SSs of *V. vulnificus* play a role in intra-species targeting *in vivo*. To further explore these results, we repeated the assay with an increased ratio of attacker to prey of 10:1 (Fig. 4B). This assay resulted in an even greater reduction of 99-743 when challenged with 106-2A, ΔT6SS1 and ΔT6SS2, typically a >1000-fold reduction from $>10^7$ to $<10^4$ CFU/g tissue ($p < 0.001$).

As we had previously observed that *V. vulnificus* is able to kill *S.* Enteritidis in addition to other species of *Vibrio* in a T6SS-dependent manner *in vitro*, we aimed to determine whether such a phenotype could be observed *in vivo* (Church *et al*., 2016). Thus, to test inter-species targeting of the *V. vulnificus* T6SSs, we conducted *in vivo* co-culture assays employing *S.* Enteritidis CC012 as the prey strain at an attacker to prey ratio of 5:1 (Fig. 4C). Similar to the killing of *V. vulnificus* 99-743 seen previously, the attacker strain *V. vulnificus* 106-2A was able to reduce *S.* Enteritidis levels from $>10^7$ to $<10^6$ CFU/g tissue following *in vivo* co-culture. Both attacking strains, ΔT6SS1 and ΔT6SS2, also killed *S.* Enteritidis to comparable levels as the wild-type attacker strain 106-2A. Fascinatingly, the ΔT6SS1/2 attacker strain had no observable killing phenotype towards the *S.* Enteritidis prey strain. As previously noted for 99-743, increasing the attacker to prey ratio from 5:1 to 10:1 resulted in a significant, dose-dependent reduction in *S.* Enteritidis within oyster stomach tissue, with levels being reduced from $>10^7$ to $<10^4$ CFU/g oyster tissue ($p < 0.05$) (Fig. 4D). In this study, we have demonstrated that *V. vulnificus* strains are capable of killing neighbouring bacterial species using both T6SS1 and T6SS2 at 21°C *in vivo* as demonstrated *in vitro*. Competition with a ΔT6SS1/2 mutant confirmed that this killing was T6SS-dependent.

Discussion

Relevant *in vivo* models are the idyll of studying host–bacteria interactions. While previous studies have

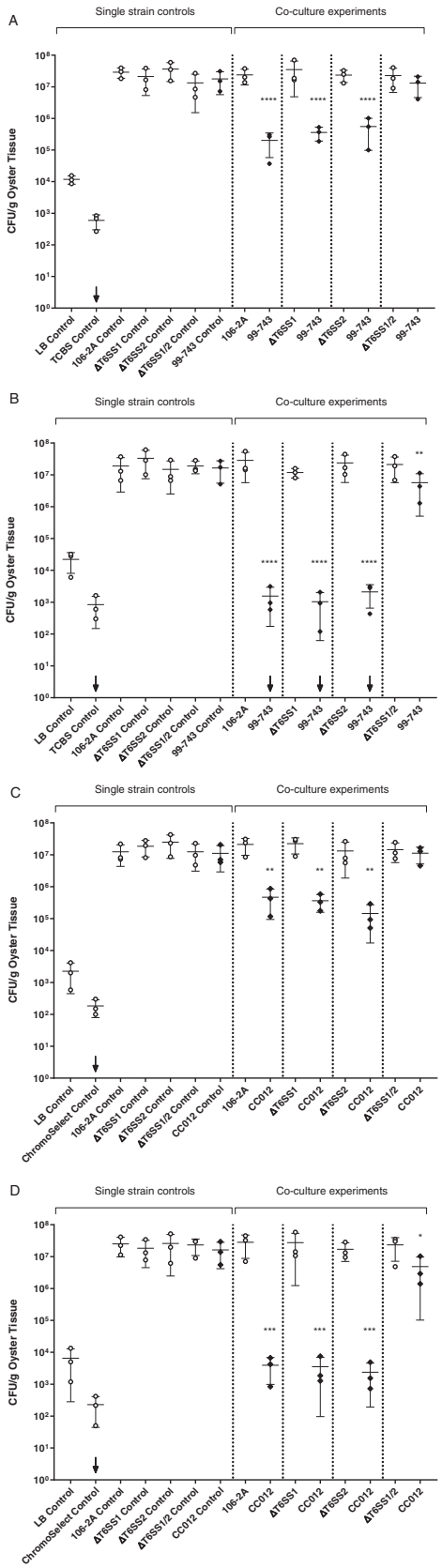

attempted to generate oyster models of bacteria uptake, these models have suffered from reproducibility issues, along with an inability to achieve sufficiently adequate levels of uptake (Morrison *et al*., 2011; Morrison *et al*., 2012; Froelich and Oliver, 2013). Our unique model of AMS, used here as a vector for delivery of bacteria to oysters, provides a robust and relevant model for studies requiring bacteria–oyster interaction. We utilized this model to demonstrate its suitability for investigating intra and inter-species bacterial killing, reporting for the first time an *in vivo* phenotype for the T6SSs of *V*. *vulnificus*.

The roles of T6SSs of bacteria are multifaceted, providing a selective advantage to bacteria possessing these systems over those without, through the secretion of 'effector' proteins involved in disabling target cells. Several bacterial pathogens, such as *V*. *cholerae*, also secrete effectors that are involved in virulence, although no one factor is uniquely correlated with virulence (Pukatzki *et al*., 2006; Burtnick *et al*., 2011; Baker-Austin and Oliver, 2018). Given that the T6SS2 is present in all sequenced strains of *V*. *vulnificus* to date, we assessed the potential role of this T6SS in virulence in a *D*. *discoideum* eukaryotic model at 21°C (Solomon *et al*., 2000). As shellfish digestive glands are highly polymicrobial, we hypothesised that T6SS1 and T6SS2 may target eukaryotic microorganisms at this lower temperature. Anti-eukaryotic T6SS activity has been observed in a number of microorganisms, such as the antifungal T6SS effectors, Tfe1 and Tfe2, of *Serratia marcescens* (Trunk *et al*., 2018). However, our data demonstrated that unlike *V*. *cholerae*, neither the wild-type nor the T6SS mutants of *V*. *vulnificus* exhibited any anti-eukaryotic

Fig. 4. *Vibrio vulnificus* 106-2A has intra-/inter-species killing activity at 21°C *in vivo*. Attacker *V*. *vulnificus* strains (106-2A, ΔT6SS1, ΔT6SS2, ΔT6SS1/2) were individually co-cultured in oysters with either prey *V*. *vulnificus* 99-743 or prey *Salmonella* Enteritidis CC012 for 24 h at 21°C at attacker to prey ratios of 5:1 and 10:1. In parallel to co-culture oysters, single strain uptake and bacteria-free controls were assessed to ensure bacteria were being ingested as expected. Each point represents the mean of six technical oyster replicates (n = 3). Horizontal bars represent the mean, error bars represent the standard deviation. Attacking strains are represented with circles, prey strains with diamonds. Vertical dotted lines separate attacker, prey and control values into their respective groups. Downward arrows indicate that some oysters were below the 100 CFU/g tissue limit of detection. A. *Vibrio vulnificus* 106-2A, ΔT6SS1, ΔT6SS2 and ΔT6SS1/2 co-culture with *V*. *vulnificus* 99-743 at a 5:1 ratio. B. *Vibrio vulnificus* 106-2A, ΔT6SS1, ΔT6SS2 and ΔT6SS1/2 co-culture with *V*. *vulnificus* 99-743 at a 10:1 ratio. C. *Vibrio vulnificus* 106-2A, ΔT6SS1, ΔT6SS2 and ΔT6SS1/2 co-culture with *S*. Enteritidis CC012 at a 5:1 ratio. D. *Vibrio vulnificus* 106-2A, ΔT6SS1, ΔT6SS2 and ΔT6SS1/2 co-culture with *S*. Enteritidis CC012 at a 10:1 ratio. Statistical significant reduction in prey strain CFU/g tissue was determined through comparing prey counts from co-culture oysters to prey counts from the single-strain prey cohort using a nested one-way analysis of variance with Dunnett's multiple comparisons test. * $p < 0.05$, ** $p < 0.01$, *** $p < 0.001$, **** $p < 0.0001$.

properties in this model, reinforcing the hypothesis that these T6SSs are predominantly antibacterial.

Examination of *V. vulnificus* genomes has identified two T6SSs, termed T6SS1 and T6SS2 (Church *et al*., 2016). While all sequenced *V. vulnificus* strains possess a T6SS2, only a subset possesses a T6SS1. *in vitro* competition assays have previously demonstrated that T6SS1$^+$ strains exhibit antibacterial activity against T6SS1$^-$ strains, suggesting a role for the T6SS1 in bacterial competition (Church *et al*., 2016). In this paper, we demonstrate that both the T6SS1 and T6SS2 are active at environmental temperatures and that both facilitate intra- and inter-species killing. Interestingly, our data show that *V. vulnificus* 106-2A is able to target and kill *V. vulnificus* 99-743 in a T6SS2-dependent manner, despite 99-743 also being T6SS2$^+$. This may be due to 106-2A encoding T6SS2 effectors not found in 99-743, against which it does not express cognate immunity proteins. This has been demonstrated previously in *V. cholerae* where genomic analysis of a panel of *V. cholerae* strains revealed that strains possessed a variety of effectors not always identical to one another (Unterweger *et al*., 2014). Strains with dissimilar effector panels were labelled 'incompatible' and shown to compete with one another. Similarly, *V. alginolyticus* contains an array of 'orphan' effectors neighbouring mobile elements obtained from other marine bacteria through horizontal gene transfer (Salomon *et al*., 2015). It is thus possible that *V. vulnificus* 106-2A has horizontally acquired T6SS2 effector proteins to which *V. vulnificus* 99-743 does not possess the cognate immunity protein, rendering 99-743 vulnerable to T6SS2-mediated killing. Future work will be required to confirm this is the case in *V. vulnificus*.

Although the large majority of seafood-related deaths in the United States are attributed to *V. vulnificus* with several reported cases having a fatality rate exceeding 50%, the clinical incidence is low given the prevalence of *V. vulnificus* in shellfish coupled with the quantity consumed. Of between 18.5 and 26.5 million Americans at risk, fewer than 100 cases are reported annually (Warner and Oliver, 2008). Historical reports demonstrate a varied population structure of *V. vulnificus* within oysters, and it may well be that the T6SS1 and T6SS2 systems contribute to a reduction in numbers of strains that are clinically isolated. We further demonstrated *in vitro* inter-species killing potential of both T6SSs by co-culture assays utilizing *S*. Enteritidis CC012 as prey. *Salmonella* species have been identified in up to 8.6% of domestic oysters within the United States, although there are few *Salmonella* outbreaks associated with fish or shellfish documented in the literature (Morrison *et al*., 2012). Whether this is a reflection on detection techniques or in part due to inter-species bacterial competition, or both, remains to be resolved.

While the *in vitro* data presented in this paper empirically demonstrate the competitive ability of *V. vulnificus*, the experimental approach of using AMS to replicate an *in vivo* scenario supports this competitive behaviour *in vivo*. The AMS model provides a means for reproducible and efficient uptake of high numbers of bacteria by oysters. Previous studies into the uptake of *V. vulnificus* or *S*. Enteritidis by oysters have relied on the filtration of planktonic bacteria added to oyster tank water. Such research resulted in levels no higher than 10^5 CFU/g tissue (Srivastava *et al*., 2009; Froelich *et al*., 2010; Morrison *et al*., 2011; Morrison *et al*., 2012; Froelich and Oliver, 2013; Pu *et al*., 2018). NMS as a vehicle to promote *V. vulnificus* uptake by oysters was first documented by Froelich *et al*. (2013), where bacteria were incorporated into NMS generated from seawater. Despite successful incorporation of bacteria into NMS, a number of factors limiting incorporation and subsequent oyster uptake levels were proposed. To resolve these issues, we developed an AMS model using the diatom, *T. pseudonana* CCMP 1335, as a substrate for aggregate formation as it had previously been shown that marine snow can be generated using a range of diatom species (Grossart and Ploug, 2001; Flintrop *et al*., 2018). Utilizing *T. pseudonana* in AMS at specific concentrations led to consistent aggregate formation, with reproducible incorporation levels of *V. vulnificus* and *S*. Enteritidis, 10,000-fold greater than those observed with NMS. Exposure of oysters to AMS resulted in extremely rapid ingestion of bacterial cultures to levels of 10^6–10^8 CFU/g tissue, >1000-fold higher than other oyster uptake experiments published to date (Froelich and Oliver, 2013). This study has demonstrated that AMS is a versatile and highly reproducible model for facilitating rapid and high-level uptake of bacteria into oysters compared with NMS or simple tank-inoculation practices.

We employed our AMS model to prove that *V. vulnificus* T6SS1 and T6SS2 have intra- and inter-species antibacterial activity in an oyster *in vivo* model. This is the first study to demonstrate T6SS *in vivo* activity in oysters facilitated by AMS. Our work suggests that both T6SS1 and T6SS2 are responsible for killing at environmental temperatures around 21°C. It will be of interest to determine the effective environmental ranges of the T6SS *in vivo* through further studies and the control that other regulators such as salinity have over the activity of the two systems. Interestingly, we observed more effective killing of prey bacteria *in vivo* compared with the *in vitro* plate-based assays. While this may be simply explained by the greater ratio of attacker to prey, another reason for this may lie in the regulation of the T6SSs, of which little is still fully understood. As T6SSs are involved in microbial competition, it is possible that they are upregulated under conditions where increased competition is required, such as

nutrient-limiting environments. Specifically, recently identified roles for bacterial T6SSs have been in the acquisition of essential micronutrients. *Burkholderia thailandensis*, *Pseudomonas aeruginosa* and *Yersinia pseudotuberculosis* T6SSs have all demonstrated secretion of effectors involved in nutrient acquisition, including manganese scavengers, zinc-binding proteins and iron-chelators (Liu *et al*., 2015; Si *et al*., 2017a; Si *et al*., 2017b).

In conclusion, this study has further characterized the activity of the T6SSs of *V*. *vulnificus* and has identified thermoregulatory conditions under which these are active. These are the first published findings confirming T6SS2 antibacterial activity of *V*. *vulnificus*. This study has also developed a widely applicable AMS model which facilitates incorporation of high numbers of bacterial that can subsequently be ingested by oysters for *in vivo* studies. Such studies demonstrated that both the T6SS1 and T6SS2 of *V*. *vulnificus* are active *in vivo* and capable of intra- and inter-species killing. Future work will look at expanding these competition assays to further understand T6SS regulation, activity and mode of action both *in vitro* and *in vivo*.

Experimental procedures

Culture conditions

Vibrio vulnificus and *S*. Enteritidis, were routinely cultured at 37°C in Luria-Bertani (LB) broth (Oxoid). *Vibrio vulnificus* plate cultures were maintained on TCBS agar (Oxoid) at room temperature. *Salmonella* Enteritidis plate cultures were maintained on ChromoSelect *Salmonella* chromogenic media (Merck). Where necessary, antibiotics were added at the following concentrations: ampicillin (50 μg/ml), kanamycin (100 μg/ml), trimethoprim (100 μg/ml) and chloramphenicol (35 μg/ml for *Escherichia coli*, 10 μg/ml for *V*. *vulnificus*). All utilized strains, plasmids and primers are listed in Tables S1–S3.

Dictyostelium discoideum (accession number: DBS0235542) was ordered via DictyBase (Fey *et al*., 2013) and received growing on a lawn of *E*. *coli* B/r. Axenic cultures were generated by inoculating 30 ml HL5 media (Formedium™) supplemented with ampicillin (100 μg/ml) and streptomycin (300 μg/ml) with an inoculating loop of *D*. *discoideum* fruiting bodies. Cultures were incubated at 21°C, 180 rpm for 2–3 days. Before cultures exceeded 10^6 cells/ml, 1 ml of culture was used to inoculate 30 ml of antibiotic-free HL5. Cultures were incubated at 21°C, 180 rpm for 2–3 days and routinely checked for contamination.

Generation of T6SS in-frame deletion mutants

V. *vulnificus* ΔT6SS1, ΔT6SS2 and ΔT6SS1/2 were generated through in-frame deletion of *hcp1* and *hcp2*. Upstream and downstream flanking regions for both genes were PCR-amplified and cloned into pGEM-T Easy for sequencing (Eurofins). Once confirmed, regions were enzymatically excised, purified and ligated into allelic exchange vector, pDM4 (Milton *et al*., 1996). Constructs pDM4-Δ*hcp1* and pDM4-Δ*hcp2* were transformed into *E*. *coli* S17-1 λ *pir* and triparentally conjugated into *V*. *vulnificus* 106-2A using conjugal donor, *E*. *coli* HB101 pRK2013. First crossover integrants were selected for on TCBS agar supplemented with chloramphenicol. To promote a second crossover event, first crossovers were plated on LB agar supplemented with 10% sucrose and incubated at 37°C for 24 h. Second crossover mutants were confirmed through PCR and sequenced to confirm the insertion was in-frame. Expression of downstream genes was confirmed using RT-PCR.

RNA extraction and RT-PCR

RNA was extracted from bacterial cultures using the RiboPure™-Bacteria kit (ThermoFisher) according to the manufacturer's instructions. 50 ng random hexamers were mixed with 1 μg total RNA, 1 μl 10 mM dNTPs and MiliQ H_2O to 13 μl. This solution was incubated at 65°C for 5 min and incubated on ice for a further 5 min. Following incubation, the following reagents were added to the microcentrifuge tube: 4 μl 5× First-Strand Buffer, 1 μl 0.1 M DTT, 1 μl RNaseOUT™, 1 μl SuperScript™ III RT (all reagents Invitrogen). The solution was incubated at 25°C for 5 min before being incubated for a further 60 min at 50°C for cDNA generation.

Generation of antibiotic-resistant V. vulnificus *strains*

To enable antibiotic selection of *V*. *vulnificus* attacker and prey strains following co-culture, plasmids conferring antibiotic resistance were electroporated into *V*. *vulnificus* and selected for on LB supplemented with either kanamycin or trimethoprim. pVv3-Kan was utilized to confer kanamycin resistance to attacker strains (Klevanskaa *et al*., 2014), and pVv3-Tmp was employed to confer resistance to trimethoprim for prey strains. Electroporation was performed according to the protocol presented in Klevanskaa *et al*. (2014). As selective chromogenic media was utilized for *Salmonella* selection, there was no need to generate antibiotic-resistant *Salmonella* strains.

In vitro *co-culture competition assays*

Attacker and prey strain cultures were subcultured in 30 ml fresh selective LB to an OD_{590nm} of 0.03 and grown to an OD_{590nm} of 1 before being adjusted to an OD_{590nm} of 0.8. Cultures were pelleted, washed twice with phosphate-buffered saline (PBS) to remove any antibiotics before

being resuspended in PBS at an OD_{590nm} of 0.8. Attacker and prey strains were combined at a ratio of 3:1 and 25 μl spotted onto LB agar. Following incubation, bacterial spots were excised using a scalpel and resuspended in 1 ml PBS. Tenfold serial dilutions were performed and triplicate 10 μl spots for each dilution were plated on the required selective media. Plates were incubated at 37°C and the average CFU/ml was calculated the following day.

Dictyostelium discoideum *plaque-forming assays*

Overnight bacterial cultures were pelleted by centrifugation and resuspended to an OD_{590nm} of 5.5 in KK2 buffer. Of note, 1 ml *D. discoideum* culture was pelleted by centrifugation at 2500 rpm for 5 min. Pelleted cells were washed once with KK2 buffer, centrifuged for a further 5 min and resuspended in 1 ml KK2 buffer. Resuspended *D. discoideum* AX3 were added to 1 ml of bacterial culture at a final concentration of 10^2 cells/ml. Of note, 200 μl of the resulting suspension was spread on SM agar and incubated at 21°C for 3–5 days to allow plaque formation (Pukatzki *et al*., 2006).

Generating natural and AMS

NMS was generated by combining 1 l collected seawater (Dawlish Warren) with 1 ml bacterial culture adjusted to an OD_{590nm} of 0.8 and 1 μg/L hyaluronic acid (Fisher). Tubes were rolled for 24 h at 8 rpm and 21°C. AMS was generated by combining 1 l artificial seawater (20 ppt salinity), with 1 ml TP 1800 (10^9 cells) (Reed Mariculture), 1 ml bacterial culture adjusted to an OD_{590nm} of 0.8 and 1 μg/L hyaluronic acid (Fisher). Tubes were rolled for 24 h at 8 rpm and 21°C.

Enumerating bacterial incorporation into marine snow

Marine snow was vacuum-filtered through qualitative filter paper No. 6 (Whatman) with a pore size of 3 μm. Non-aggregated bacteria are too small to be retained by the filter paper. Any cells incorporated into larger marine snow aggregates were retained on the filter paper. Filtered aggregates were resuspended in 50 ml PBS and vortexed vigorously to disrupt the aggregates. Samples were centrifuged to pellet the material, resuspended in 10 ml PBS and serially diluted 10-fold for spread-plate enumeration on LB, TCBS or ChromoSelect agar. Plates were incubated at 37°C overnight and CFU/g marine snow calculated the following day.

Scanning electron microscopy

Marine snow samples were fixed in 2% glutaraldehyde and 2% paraformaldehyde in 0.1 M Pipes buffer pH 7. Fixed samples were transferred onto a 0.1 μm polycarbonate filter and washed for 5 min in Pipes buffer for a total of three times. Aggregates attached to the filter were dehydrated using an ethanol gradient. The filter was incubated for 3 min in hexamethyldisilazane before air-drying. Dried filters were mounted onto an aluminium sample pin using carbon conductive tabs. Samples were then sputter-coated with 10 nm gold/palladium (80/20) and imaged using a JEOL JSM 6390 LV scanning electron microscope operated at 5 kV. Images were contrast-adjusted and false-coloured using Adobe Photoshop CC 2019 V20.0. Raw images can be seen in Figure S3A–D.

Oyster husbandry

Pacific oysters (*Crassostrea gigas*) were obtained from Lindisfarne oyster farm (Lindisfarne oysters, Northumberland). Upon arrival, oysters were scrubbed and placed in static holding tanks containing 20 ppt salinity artificial seawater at 21°C. Oysters were maintained at the University of Exeter in the Aquatic Resources Centre under their prescribed oyster husbandry protocols. Oysters were allowed to acclimatize for 5 days. Water was changed daily, and oysters were fed with 250 μl TP 1800® (Reed Mariculture) every other day.

In vivo *oyster exposure assays*

Oysters were maintained in individual 5 l holding aquaria at 21°C. AMS was added to the holding tanks taking care to not disrupt the aggregates. Six oysters were utilized for each exposure. Oysters were left to filter and ingest the inoculated marine snow for 24 h. A circulatory current was generated by the presence of an air stone to prevent aggregate settling. Following exposure, oysters were removed from their tanks and briefly cleaned with 70% ethanol to remove non-ingested microorganisms. Using a flame-sterilized knife, oysters were shucked and the stomachs excised. Samples were weighed before being suspended in 10 ml PBS and homogenized for 3 min in a Stomacher 400 (Seward). The resulting homogenate was filtered through a 40-μm cell strainer (Merck) into a clean 50-ml falcon tube to remove tissue debris. The resulting filtrate was serially diluted 10-fold in PBS. Of note, 100 μl of each dilution was spread on LB agar and incubated overnight at 37°C. The following day, all colonies were replica plated onto *Vibrio* selective TCBS and incubated overnight at 37°C. Colonies were then enumerated based off colour and recorded for CFU/g tissue calculations. Assays involving *Salmonella* were not plated onto LB but instead straight onto *Salmonella*-selective ChromoSelect agar.

Acknowledgements

The authors would like to thank Dr Stefan Hertwig for the donation of the pVv3-Kan and pVv3-Kan-Tmp plasmids and Dr Christian Hacker for his technical assistance obtaining the SEM images. This research was funded by The Natural Environment Research Council, grant number NE/L002434/1.

Author contributions

C.L.H. and S.L.M. designed the experiments. Both authors contributed to the preparation of the manuscript. S.L.M. conceived the study and obtained the funding.

References

Baker-Austin, C., and Oliver, J.D. (2018) *Vibrio vulnificus*: new insights into a deadly opportunistic pathogen. *Environ Microbiol* **20**: 423–430.

Baker-Austin, C., Trinanes, J.A., Taylor, N.G.H., Hartnell, R., Siitonen, A., Martinez-Urtaza, J. (2012) Emerging *Vibrio* risk at high latitudes in response to ocean warming. *Nat Clim Chang* **3**: 73–77.

Baker-Austin, C., Trinanes, J., Gonzalez-Escalona, N., and Martinez-Urtaza, J. (2017) Non-cholera *Vibrios*: the microbial barometer of climate change. *Trends Microbiol* **25**: 76–84.

Beatty, N.L., Marquez, J., and Al Mohajer, M. (2017) Skin manifestations of primary *Vibrio vulnificus* septicemia. *Am J Trop Med Hyg* **97**: 1–2.

Berni, B., Soscia, C., Djermoun, S., Ize, B., and Bleves, S. (2019) A type VI secretion system trans-kingdom effector is required for the delivery of a novel antibacterial toxin in *Pseudomonas aeruginosa*. *Front Microbiol* **10**: 1218.

Bondad-Reantaso, M.G., Subasinghe, R.P., Arthur, J.R., Ogawa, K., Chinabut, S., Adlard, R., *et al*. (2005) Disease and health management in Asian aquaculture. *Vet Parasitol* **132**: 249–272.

Bruto, M., James, A., Petton, B., Labreuche, Y., Chenivesse, S., Alunno-Bruscia, M., *et al*. (2017) *Vibrio crassostreae*, a benign oyster colonizer turned into a pathogen after plasmid acquisition. *ISME J* **11**: 1043–1052.

Burtnick, M.N., Brett, P.J., Harding, S.V., Ngugi, S.A., Ribot, W.J., Chantratita, N., *et al*. (2011) The cluster 1 type VI secretion system is a major virulence determinant in *Burkholderia pseudomallei*. *Infect Immun* **79**: 1512–1525.

Cascales, E., and Cambillau, C. (2012) Structural biology of type VI secretion systems. *Philos Trans R Soc Lond B Biol Sci* **367**: 1102–1111.

CDC n.d. Oysters and vibriosis | features | CDC.

Chiang, C., Chiang, S.-R., and Chuang, Y.-C. (2003) *Vibrio vulnificus* infection: clinical manifestations, pathogenesis, and antimicrobial therapy. *J Microbiol Immunol Infect* **36**: 81–88.

Church, S.R., Lux, T., Baker-Austin, C., Buddington, S.P., and Michell, S.L. (2016) *Vibrio vulnificus* type 6 secretion system 1 contains anti-bacterial properties. *PLoS One* **11**: e0165500.

Deeb, R., Tufford, D., Scott, G., Gooch Moore, J., and Dow, K. (2018) Impact of climate change on *Vibrio vulnificus* abundance and exposure risk. *Estuar Coasts* **41**: 2289–2303.

Dubert, J., Nelson, D.R., Spinard, E.J., Kessner, L., Gomez-Chiarri, M., Costa, F.., *et al*. (2016) Following the infection process of vibriosis in Manila clam (*Ruditapes philippinarum*) larvae through GFP-tagged pathogenic *Vibrio* species. *J Invertebr Pathol* **133**: 27–33.

Fey, P., Dodson, R.J., Basu, S., and Chisholm, R.L. (2013) *One Stop Shop for Everything* Dictyostelium*: dictyBase and the Dicty Stock Center in 2012*. Totowa, NJ: Humana Press, pp. 59–92.

Flintrop, C.M., *et al*. (2018) Embedding and slicing of intact *in situ* collected marine snow. *Limnol Oceanogr Methods* **16**: 339–355.

Froelich, B.A., and Noble, R.T. (2014) Factors affecting the uptake and retention of *Vibrio vulnificus* in oysters. *Appl Environ Microbiol* **80**: 7454–7459.

Froelich, B., and Oliver, J. (2013) Increases in the amounts of *Vibrio* spp. in oysters upon addition of exogenous bacteria. *Appl Environ Microbiol* **79**: 5208–5213.

Froelich, B., Ringwood, A., Sokolova, I., and Oliver, J. (2010) Uptake and depuration of the C- and E-genotypes of *Vibrio vulnificus* by the eastern oyster (*Crassostrea virginica*). *Environ Microbiol Rep* **2**: 112–115.

Froelich, B., Ayrapetyan, M., and Oliver, J.D. (2013) Integration of *Vibrio vulnificus* into marine aggregates and its subsequent uptake by *Crassostrea virginica* oysters. *Appl Environ Microbiol* **79**: 1454–1458.

Froelich, B.A., Phippen, B., Fowler, P., Noble, R.T., and Oliver, J.D. (2017) Differences in abundances of total *Vibrio* spp., *V. vulnificus*, and *V. parahaemolyticus* in clams and oysters in North Carolina. *Appl Environ Microbiol* **83**: e02265-16.

Fu, Y., Ho, B.T., and Mekalanos, J.J. (2018) Tracking *Vibrio cholerae* cell-cell interactions during infection reveals bacterial population dynamics within intestinal microenvironments. *Cell Host Microbe* **23**: 274–281.e2.

Grossart, H.-P., and Ploug, H. (2001) Microbial degradation of organic carbon and nitrogen on diatom aggregates. *Limnol Oceanogr* **46**: 267–277.

Grossart, H.-P., Kiørboe, T., Tang, K., and Ploug, H. (2003) Bacterial colonization of particles: growth and interactions. *Appl Environ Microbiol* **69**: 3500–3509.

Ho, B., Dong, T., and Mekalanos, J. (2014) A view to a kill: the bacterial type VI secretion system. *Cell Host Microbe* **15**: 9–21.

Hsieh, P.-F., Lu, Y.-R., Lin, T.-L., Lai, L.-Y., and Wang, J.-T. (2019) *Klebsiella pneumoniae* type VI secretion system contributes to bacterial competition, cell invasion, type-1 fimbriae expression, and in vivo colonization. *J Infect Dis* **219**: 637–647.

Ishikawa, T., Sabharwal, D., Bröms, J., Milton, D.L., Sjöstedt, A., Uhlin, B.E., and Wai, S.N. (2012) Pathoadaptive conditional regulation of the type VI secretion system in *Vibrio cholerae* O1 strains. *Infect Immun* **80**: 575–584.

Jones, M., and Oliver, J. (2009) *Vibrio vulnificus*: disease and pathogenesis. *Infect Immun* **77**: 1723–1733.

Kaspar, C., and Tamplin, M. (1993) Effects of temperature and salinity on the survival of *Vibrio vulnificus* in seawater and shellfish. *Appl Environ Microbiol* **59**: 2425–2429.

Kim, D.M., Jung, S.I., Jang, H.C., Lee, C.S., Lee, S.H., Yun, N.R., *et al*. (2011) *Vibrio vulnificus* DNA load and mortality. *J Clin Microbiol* **49**: 413–415.

Kiørboe, T., Andersen, K.P., and Dam, H.G. (1990) Coagulation efficiency and aggregate formation in marine phytoplankton. *Mar Biol* **107**: 235–245.

Kiørboe, T., Tang, K., Grossart, H.-P., and Ploug, H. (2003) Dynamics of microbial communities on marine snow aggregates: colonization, growth, detachment, and grazing mortality of attached bacteria. *Appl Environ Microbiol* **69**: 3036–3047.

Klevanskaa, K., Bier, N., Stingl, K., Strauch, E., and Hertwig, S. (2014) pVv3, a new shuttle vector for gene expression in *Vibrio vulnificus*. *Appl Environ Microbiol* **80**: 1477–1481.

Lacoste, A., Jalabert, F., Malham, S., Cueff, A., Gélébart, F., Cordevant, C., *et al*. (2001) A *Vibrio splendidus* strain is associated with summer mortality of juvenile oysters *Crassostrea gigas* in the bay of Morlaix (North Brittany, France). *Dis Aquat Org* **46**: 139–145.

Liu, L., Hao, S., Lan, R., Wang, G., Xiao, D., Sun, H., and Xu, J. (2015) The type VI secretion system modulates flagellar gene expression and secretion in *Citrobacter freundii* and contributes to adhesion and cytotoxicity to host cells. *Infect Immun* **83**: 2596–2604.

Menon, M., Yu, P., Iwamoto, M., and Painter, J. (2014) Pre-existing medical conditions associated with *Vibrio vulnificus* septicaemia. *Epidemiol Infect* **142**: 878–881.

Milton, D.L., O'toole, R., Horstedt, P., Horstedt, H., and Wolf-Watz, H. (1996) Flagellin A is essential for the virulence of *Vibrio anguillarum*. *J Bacteriol* **178**: 1310–1319.

Miyata, S.T., Kitaoka, M., Brooks, T.M., McAuley, S.B., and Pukatzki, S. (2011) *Vibrio cholerae* requires the type VI secretion system virulence factor VasX to kill *Dictyostelium discoideum*. *Infect Immun* **79**: 2941–2949.

Morrison, C.M., Armstrong, A.E., Evans, S., Mild, R.M., Langdon, C.J., and Joens, L.A. (2011) Survival of *Salmonella* Newport in oysters. *Int J Food Microbiol* **148**: 93–98.

Morrison, C.M., Dial, S.M., Day, W.A., Joens, L.A., and Joens, L.A. (2012) Investigations of *Salmonella enterica* serovar Newport infections of oysters by using immunohistochemistry and knockout mutagenesis. *Appl Environ Microbiol* **78**: 2867–2873.

Oliver, J. (2005) Wound infections caused by *Vibrio vulnificus* and other marine bacteria. *Epidemiol Infect* **133**: 383–391.

Passow, U., Ziervogel, K., Asper, V., and Diercks, A. (2012) Marine snow formation in the aftermath of the Deepwater horizon oil spill in the Gulf of Mexico. *Environ Res Lett* **7**: 035301.

Pu, M., Duriez, P., Arazi, M., and Rowe-Magnus, D.A. (2018) A conserved tad pilus promotes *Vibrio vulnificus* oyster colonization. *Environ Microbiol* **20**: 828–841.

Pukatzki, S., Ma, A.T., Sturtevant, D., Krastins, B., Sarracino, D., Nelson, W.C., *et al*. (2006) Identification of a conserved bacterial protein secretion system in *Vibrio cholerae* using the *Dictyostelium* host model system. *Proc Natl Acad Sci U S A* **103**: 1528–1533.

Pukatzki, S., Ma, A.T., Revel, A.T., Sturtevant, D., and Mekalanos, J.J. (2007) Type VI secretion system translocates a phage tail spike-like protein into target cells where it cross-links Actin. *Proc Natl Acad Sci U S A* **104**: 15508–15513.

Ray, A., Schwartz, N., Souza Santos, M., Zhang, J., Orth, K., and Salomon, D. (2017) Type VI secretion system MIX-effectors carry both antibacterial and anti-eukaryotic activities. *EMBO Rep* **18**: 1978–1990.

Rico, A., Satapornvanit, K., Haque, M.M., Min, J., Nguyen, P.T., Telfer, T.C., and van den Brink, P.J. (2012) Use of chemicals and biological products in Asian aquaculture and their potential environmental risks: a critical review. *Rev Aquac* **4**: 75–93.

Salomon, D., Gonzalez, H., Updegraff, B.L., and Orth, K. (2013) *Vibrio parahaemolyticus* type VI secretion system 1 is activated in marine conditions to target bacteria, and is differentially regulated from system 2. *PLoS One* **8**: e61086.

Salomon, D., Klimko, J.A., Trudgian, D.C., Kinch, L.N., Grishin, N.V., Mirzaei, H., and Orth, K. (2015) Type VI secretion system toxins horizontally shared between marine bacteria. *PLoS Pathog* **11**: e1005128.

Si, M., Wang, Y., Zhang, B., Zhao, C., Kang, Y., Bai, H., *et al*. (2017a) The type VI secretion system engages a redox-regulated dual-functional heme transporter for zinc acquisition. *Cell Rep* **20**: 949–959.

Si, M., Zhao, C., Burkinshaw, B., Zhang, B., Wei, D., Wang, Y., *et al*. (2017b) Manganese scavenging and oxidative stress response mediated by type VI secretion system in *Burkholderia thailandensis*. *Proc Natl Acad Sci* **114**: E2233–E2242.

SOFIA State of fisheries and aquaculture in the world 2018.

Solomon, J.M., Rupper, A., Cardelli, J.A., and Isberg, R.R. (2000) Intracellular growth of *Legionella pneumophila* in *Dictyostelium discoideum*, a system for genetic analysis of host-pathogen interactions. *Infect Immun* **68**: 2939–2947.

Speare, L., Cecere, A.G., Guckes, K.R., Smith, S., Wollenberg, M.S., Mandel, M.J., *et al*. (2018) Bacterial symbionts use a type VI secretion system to eliminate competitors in their natural host. *Proc Natl Acad Sci* **115**: E8528–E8537.

Srivastava, M., Tucker, M.S., Gulig, P.A., and Wright, A.C. (2009) Phase variation, capsular polysaccharide, pilus and flagella contribute to uptake of *Vibrio vulnificus* by the eastern oyster (*Crassostrea virginica*). *Environ Microbiol* **11**: 1934–1944.

Trunk, K., Peltier, J., Liu, Y.C., Dill, B.D., Walker, L., Gow, N. A.R., *et al*. (2018) The type VI secretion system deploys antifungal effectors against microbial competitors. *Nat Microbiol* **3**: 920–931.

Unterweger, D., Miyata, S.T., Bachmann, V., Brooks, T. M., Mullins, T., Kostiuk, B., *et al*. (2014) The *Vibrio cholerae* type VI secretion system employs diverse effector modules for intraspecific competition. *Nat Commun* **5**: 3549.

Vezzulli, L., Höfle, M., Pruzzo, C., Pezzati, E., and Brettar, I. (2015) Effects of global warming on *Vibrio* ecology. *Microbiol Spectr* **3**(VE-0004-2014), 1–9.

Warner, E., and Oliver, J. (2008) Population structures of two genotypes of *Vibrio vulnificus* in oysters (*Crassostrea virginica*) and seawater. *Appl Environ Microbiol* **74**: 80–85.

Supporting Information

Additional Supporting Information may be found in the online version of this article at the publisher's web-site:

Appendix S1: Supporting Information